IEEE Photonics Journal
An IEEE Photonics Society Publication

Open Access

Improved Performance of Deep Ultraviolet Photodetector From Sputtered Ga_2O_3 Films Using Post-Thermal Treatments

Volume 11, Number 6, December 2019

Hui Li
Po-Wei Chen
Shuo-Huang Yuan
Tsun-Min Huang
Sam Zhang
Dong-Sing Wuu, ***Senior Member, IEEE***

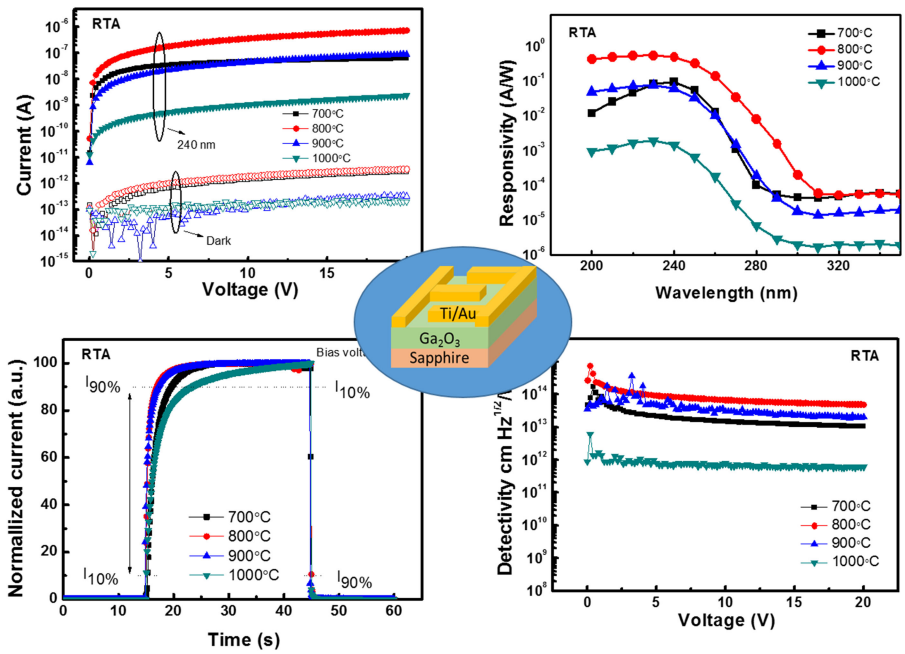

DOI: 10.1109/JPHOT.2019.2948193

Improved Performance of Deep Ultraviolet Photodetector From Sputtered Ga_2O_3 Films Using Post-Thermal Treatments

Hui Li,[1,2] Po-Wei Chen,[1] Shuo-Huang Yuan,[1] Tsun-Min Huang,[1] Sam Zhang,[2] and Dong-Sing Wuu,[1,2,3] *Senior Member, IEEE*

[1]Department of Materials Science and Engineering, National Chung Hsing University, Taichung 40227, Taiwan
[2]Centre for Advanced Thin Films and Devices, School of Materials and Energy, Southwest University, Chongqing 400715, China
[3]Innovation and Development Center of Sustainable Agriculture, National Chung Hsing University, Taichung 40227, Taiwan
[4]Research Center for Sustainable Energy and Nanotechnology, National Chung Hsing University, Taichung 40227, Taiwan

DOI:10.1109/JPHOT.2019.2948193

Manuscript received September 8, 2019; revised October 14, 2019; accepted October 16, 2019. Date of publication October 21, 2019; date of current version October 30, 2019. This work was supported in part by the Ministry of Science and Technology of Taiwan under Grants MOST 105-2221-E-005-059-MY3 and 108-2221-E-005-028-MY3, in part by the "Innovation and Development Center of Sustainable Agriculture" from The Featured Areas Research Center Program within the framework of the Higher Education Sprout Project by the Ministry of Education (MOE) in Taiwan, and in part by Fundamental Research Funds for the Central Universities at Southwest University: SWU118105. Corresponding authors: Sam Zhang; Dong-Sing Wuu (e-mail: samzhang@swu.edu.cn; dsw@nchu.edu.tw).

Abstract: The metal-semiconductor-metal photodetectors based on the sputtered gallium oxide films on sapphire substrates after various post-thermal treatments have been investigated. The photodetector performance of the furnace-annealed gallium oxide sample degraded with the increase of annealing temperature from 700 to 1000 °C, resulting from the adverse effect of the aluminum cross-diffusion and polycrystalline formation. By rapid thermal annealing at 800 °C, the gallium oxide film can achieve an optimum photodetector performance with the photo/dark current ratio of 1.78×10^5 (@5V and 230 nm), responsivity of 0.553 A/W, and fast transient response (rise/fall time: 0.2 s/0.1 s). The result is comprehensively better than the previous reports by sputtering, which demonstrates that the quasi-single-crystalline gallium oxide film via rapid thermal process has high potential for deep-ultraviolet photodetector applications.

Index Terms: Gallium oxide, photodetector, post thermal annealing, quasi-single-crystalline, diffusion.

1. Introduction

Recently, β-Ga_2O_3 (β-GO) photodetectors (PDs) have attracted intense interests in deep ultraviolet detection for military, biological and chemical analyses applications [1]–[3]. For the wavelengths below 280 nm, the deep ultraviolet PDs are very useful in the detection of trace dangerous pollutants in a confined space such as e.g., nitric oxide, due to a strong absorption in the 200–250 nm region. Various growth techniques such as molecular beam epitaxy, pulsed laser deposition, metalorganic chemical vapor deposition and sputtering have been employed to deposit GO films [4]–[6]. The sputtering is the one of reliable equipment, which can achieve a good uniformity over a large area

for industry process. To further improve the quality of sputtered films, a post-thermal treatment is usually utilized. Previous studies about sputtered GO films on sapphire substrates have been conducted [7]–[9], and an optimum annealing temperature of 1000 °C is needed to achieve the highest crystalline quality [7]. However, the aluminum diffused into the GO film during the furnace anneal process has been reported [10], and its adverse effect on PD performance is neglected. In this study, both the crystalline quality and interdiffusion are compromised and details of quasi-single-crystalline β-GO films with enhanced PD performance will be discussed.

2. Experimental Details

All the Ga_2O_3 films (120 nm in thickness) used in this study were sputtered on 2-in. c-plane sapphire (Al_2O_3) substrates at 600 °C using a 3-in. Ga_2O_3 ceramic target (4N). The applied radio-frequency (13.56 MHz) power level for the target was set as 100 W, where the working pressure of 5×10^{-3} Torr was maintained with a mixture gas of Ar/O_2 (10/2 sccm). The oxide samples were then post-annealed in a quartz tube furnace for 30 min or in a rapid thermal annealing (RTA) chamber for 1 min under various temperatures (700–1000 °C). Both the thermal treatments were performed in the air ambient. For the metal-semiconductor-metal (MSM) PD fabrication process, the Ti/Au (40/60 nm) Schottky contacts were deposited using an electron-beam evaporator and defined by conventional photolithography and lift-off techniques. The device area, finger width, and interspacing were 1.05×1.05 mm^2, 50 μm and 50 μm, respectively.

The crystallinity of the GO films was examined by X-ray diffraction (XRD, PANalytical, X'Pert Pro MRD) and the corresponding microstructure was examined by transmission electron microscopy (TEM; JEOL JEM-2100F). The elements concentration in the films and sapphire substrate were measured by time-of-flight secondary ion mass spectrometry (SIMS, IONTOF, TOF.SIMS 5). Based on the XRD pattern, the grain size was calculated by Scherrer equation. Atomic force microscopy (AFM, Agilent 5400) was used to measure the surface roughness (root mean square, RMS) of the GO films. The optical bandgap values (E_g) can be extracted through Tauc plot obtained from the transmission spectra determined by N&K analyzer (model: 1280, N and K Tech.). The band structure of the sputtered sample was determined from the results by the ultraviolet photoelectron spectroscopy measurements (ULVAC-PHI PHI 5000 Versaprobe II). The spectral responsivity (R) of the MSM PD at a bias voltage of 5 V was measured using a spectrometer (Omni3029i) with a 30 W deuterium lamp light (Zolix, LSH-D30) and a standard synchronous detection scheme measured at 60 Hz in this study. The photocurrent of the PD device was determined under an illumination wavelength (λ) of 240 nm.

3. Results and Discussion

The as-deposited GO film shows an amorphous structure with no PD response. After annealing, all samples exhibit the β-phase preferred orientations. The material properties of the GO film before and after thermal treatment are shown in Table 1. The furnace-annealed samples processed polycrystalline structure with orientations of (−201), (−402) and (−603), which belong to the (−201) group and (60–1), whereas the RTA-treated ones showed quasi-single-crystalline structure with (−201) group at 700 and 800 °C, and then transformed into polycrystals with other orientations as (400) and (002) when the annealing temperature increased to 900 and 1000 °C. The furnace-treated GO films presented better crystalline quality with small full-width-at-half-maximum (FWHM) values than those of the RTA-treated ones. The grain size and the RMS roughness of all the GO films increased, which is attributed to the supplied thermal energy to support the grain growth during the annealing process. Note that, the calculated bandgap of furnace-annealed samples continuously increased from 4.95 to 5.33 eV with increase of temperature from 700 to 1000 °C, whereas those of RTA-treated ones revealed a slight increase (5.0 eV) only at 1000 °C. This phenomenon could be resulted from the thermal-induced cross-diffusion of aluminum atoms tending to form $Al_xGa_{2-x}O_3$, which owned wider bandgap than the pure GO.

TABLE 1
Material Properties of Sputtered Gallium Oxide Films on c-Plane Sapphire Substrates With Various Annealing Treatments

	As-deposited	Furnace				RTA			
		700℃	800℃	900℃	1000℃	700℃	800℃	900℃	1000℃
Crystalline orientation	Amorphous	(-201), (-402), (-603), (60-1)				(-201), (-402), (-603)		(-201), (-402), (-603), (400),(002)	
FWHM (arcsec) @(-201) peak	-	1662.5	1327.3	1262.2	1210	2726.3	2121.8	1675.8	1421.3
Grain Size (nm)	-	17.2	21.6	22.7	23.7	10.5	13.5	17.1	20.2
RMS roughness (nm)	-	2.05	2.29	2.35	2.79	2.13	2.23	2.23	2.29
Bandgap (eV)	4.95	4.95	4.99	5.09	5.33	4.95	4.95	4.95	5.00

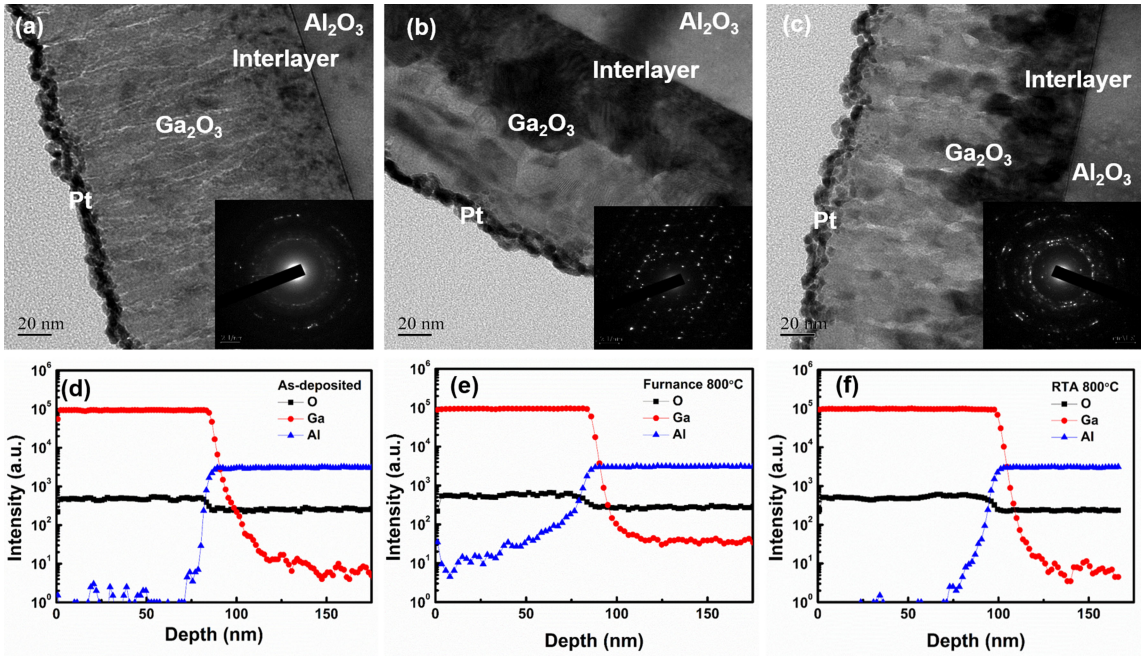

Fig. 1. Cross-sectional TEM images and SIMS figures of (a), (d) as-deposited, (b), (e) 800 °C-furnace-annealed and (c), (f) 800 °C-RTA-treated gallium oxide thin film. (Inset) SAED pattern of the same sample, respectively.

Cross-sectional TEM images and selected-area electron diffraction (SAED) patterns of the as-deposited, 800 °C-furnace-annealed and 800 °C-RTA-treated films are shown in Fig. 1. The as-deposited GO film shows an amorphous with weak polycrystalline structure as confirmed by the SEAD pattern [Fig. 1(a)]. After thermal treatments, the GO films transform into the β-monoclinic phase with (-201) group orientation. The furnace-annealed sample possesses a nearly single crystalline structure [Fig. 1(b)], whereas the RTA-treated one owns a quasi-single-crystal structure [Fig. 1(c)]. Moreover, according to the line-scan mapping results from the energy dispersive x-ray spectrometry (EDS), the average aluminum amount in the film increased from 0.43 of the as-deposited sample to 1.42 and 12 at.% for 800 and 1000 °C-furnace-annealed ones, respectively. However, only 0.52 and 1.14 at.% of aluminum amount were measured for the 800 and 1000 °C-RTA-treated GO films, indicating the less interdiffusion occurring in the RTA process. The SIMS analyses have been conducted to further examine the extent of thermal-induced diffusion.

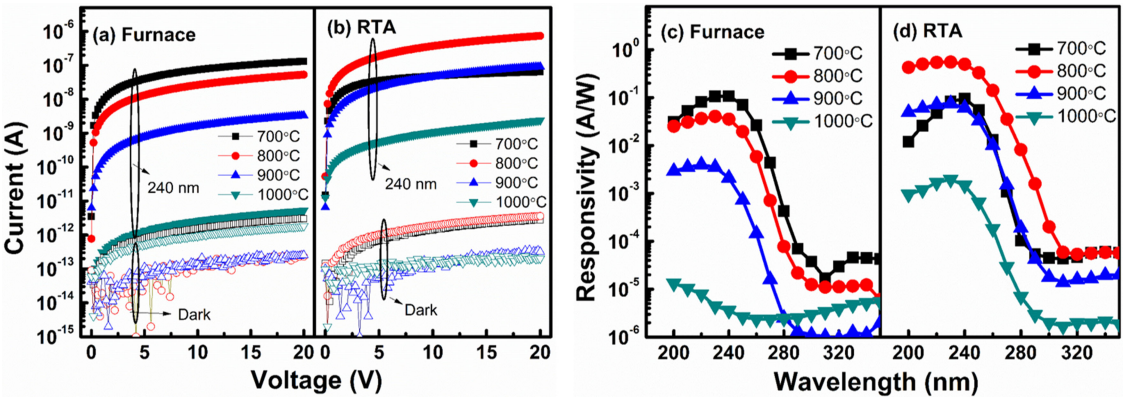

Fig. 2. (a), (b) I-V characteristics and (c), (d) spectral response of the gallium oxide metal-semiconductor-metal photodetectors with various thermal treatments. Photocurrent and responsivity were measured under 240 nm illumination and 5 V bias voltage, respectively.

As compared with the SIMS result of the as-deposited GO film [Fig. 1(d)], more serious Al diffusion was detected for the 800 °C-furnace-annealed sample where the Al extended to the GO top surface [Fig. 1(e)]. However, there was no obvious difference between the 800 °C-RTA-treated [Fig. 1(f)] and as-deposited one [Fig. 1(d)]. These results correlate well with the bandgap value variations as shown in Table 1.

Fig. 2(a) and (b) show the anneal-temperature-dependent current-voltage (I-V) characteristics of the MSM PDs fabricated with furnace- and RTA-treated GO films, respectively. When the annealing temperature increases from 700 to 1000 °C, the photocurrent (I_{ph}) of the furnace-annealed GO PD drastically decreases. The reduction of photocurrent could be attributed to the increase of GO bandgap (E_g) due to the cross-diffusion of Al atoms tending to form $Al_xGa_{2-x}O_3$, as confirmed by the EDS result from Fig. 1. With the widening of E_g, it is too deep for the energy levels of defects to activate, losing much of contribution to conductivity and photo absorption. Also, deep defects formed with the increase of diffused Al impurity will capture the generated carriers by optical absorption, leading to the reduction of I_{ph}. It was found that the dark currents (I_{dark}) of furnace-annealed-GO PDs first decreased from 700 to 800 °C and then increased with a further increase in the temperature to 1000 °C. Since these samples have no surface passivation, the dark current variation could be mainly attributed to the Schottky barrier height (SBH) at the semiconductor/metal interface [11]. For the RTA-treated GO PDs, both the I_{dark} and I_{ph} increase when the annealing temperature increases from 700 to 800 °C, and then decreased with the further temperature increase to 900 and 1000 °C as shown in Fig. 2(b). The highest on/off current contrast ratio about 10^5 can be obtained for 800 °C RTA-treated GO film, which can be attributed to the better crystal quality and fewer oxygen vacancies in the film

Fig. 2(c) and (d) show the extracted spectral responsivity for the β-GO PDs by using $R = (I_{ph} - I_{dark})/(PA)$, where P is the power density of incident light and A is the effective illuminated area [12]. These parameters are related to the reflectance and incidence of the semiconductor [13]. With the increase of annealing temperature from 700 to 1000 °C, the degraded R (@5V, $\lambda = 240$ nm) of the furnace-treated-GO PDs in the wavelength region of 200 to 280 nm could be resulted from the disorder of sputtered Ga/Al oxides due to the atomic diffusion after annealing. The blue shift in maximum R (R_{max}) also proved the increase of Eg value with more Al incorporation. On the other hand, the RTA-treated-GO PDs display a rise responsivity with the increase of annealing temperature from 700 to 800 °C. The enhancement in crystalline quality could contribute this point. However, a responsivity drop occurred for the annealing temperature higher than 800 °C. It could be attributed to the formation of the polycrystalline structure and the defects induced by the high temperature treatment. An optimum responsivity of 0.553 A/W can be achieved for

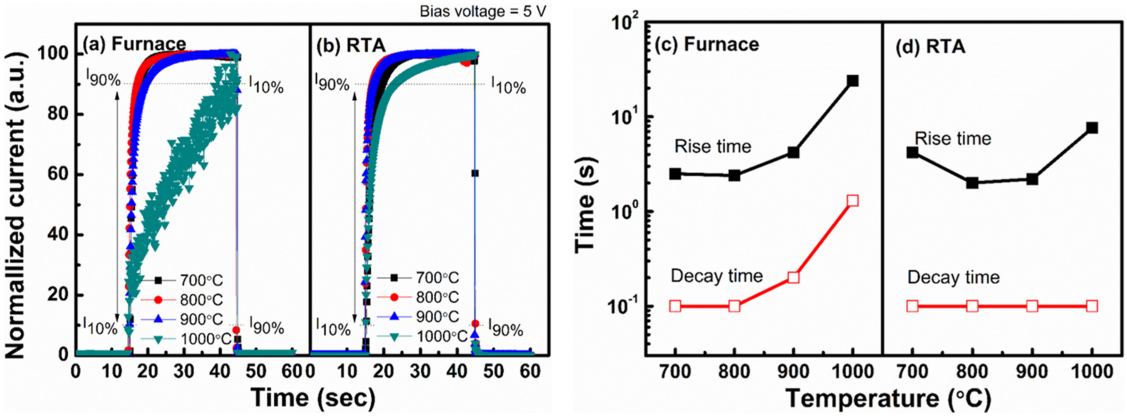

Fig. 3. Time-dependent responses (a), (b) and rise time and decay time (c), (d) for the gallium oxide metal-semiconductor-metal photodetectors with various annealing treatments.

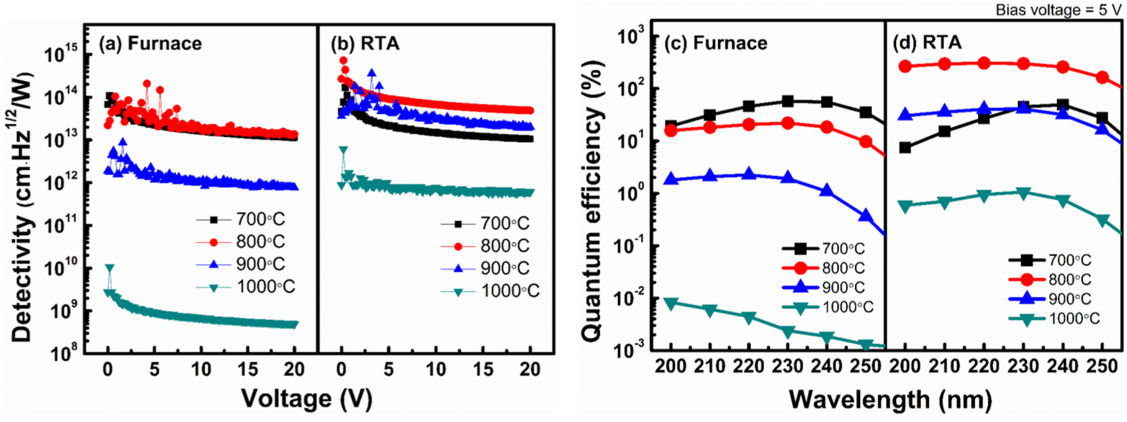

Fig. 4. Detectivities as functions of bias voltage (under 240 nm illumination) (a), (b) and quantum efficiency (c), (d) for the gallium oxide metal-semiconductor-metal photodetectors with various annealing treatments.

the 800 °C-RTA-treated GO PD, whereas a maximum responsivity of 0.107 A/W is obtained for 700 °C-furnace-annealed one.

Fig. 3(a) and (b) depict the normalized transient responses (@5 V, $\lambda = 240$ nm) of the β-GO PDs, where both the rise times (from $I_{10\%}$ to $I_{90\%}$) and decay times (from $I_{90\%}$ to $I_{10\%}$) are extracted for each PD and shown in Fig. 3(c) and (d) for furnace and RTA treatment, respectively. The obviously extended rise time and decay time for furnace-annealed-GO PDs using 900 and 1000 °C imply that there are more oxygen vacancies and other deep defects. Especially, the drastically prolonged rise time even nearly to 30 s, which indicated the adverse effects of disorder of atom arrangements resulted from server anneal-induced diffusion. There is no obvious difference in decay time ($\sim$0.1 s) among the RTA-treated GO PDs. The 800 °C-RTA-treated GO PD shows the shortest rise time, because the improved crystallinity can reduce the structural-defect-induced traps and thus the persistent photoconductivity due to the suppressed slow process of carrier detrapping. The slightly extended rise time for 900 and 1000 °C-RTA-treated GO PD could be probably ascribed to the oxygen-related hole-trap states generated at the surface of the GO film.

Fig. 4(a) and (b) show the detectivities as functions of bias voltages for the GO PDs described in Fig. 1. The detectivity refers to the minimum optical signal that can be distinguished above the noise. As the bias voltage increases, the PD detectivity decreases with the detectivity value obtained

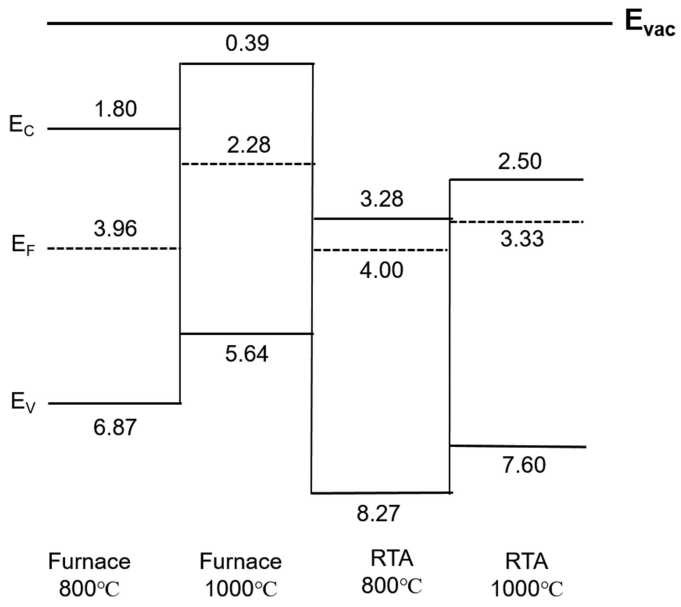

Fig. 5. Band alignment of furnace-annealed and RTA-treated Ga_2O_3 films at 800 and 1000 °C, calculated from the ultraviolet photoelectron spectroscopy measurements.

by using $D = (A^{1/2}R) / (2qI_{dark})^{1/2}$, where q is the elementary charge [14]. The detectivities (@5 V) of the furnace-annealed GO PDs decreased with the increase of the annealing temperature, especially the 1000 °C-annealed sample which showed a poor detectivity. However, those of the RTA-treated GO PDs increase when the temperature increases to 800 °C, and then decrease at 900 and 1000 °C. Obviously, the 800 °C-RTA-treated GO PD shows the optimum detectivity, which is around one to several orders of magnitude higher than that of other samples. This trend is consistent with the responsivity data presented in Fig. 2(c) and (d).

Fig. 4(c) and (d) show the quantum efficiency (QE) of the GO PD as a function of the various annealing conditions. The QE value can be extracted using $\eta = Rh\upsilon / q$, where h is the Planck constant and υ is the frequency of the emitted light [15]. Since almost no current can flow through the GO PDs with the bias voltage 5 V in a dark environment, the photocurrent (@5 V) can be regarded as photogenerated carriers under illumination. By increasing the annealing temperature, the furnace-annealed GO PDs exhibit degraded QE values. At 1000 °C, the GO PD reveals a poor QE even around 3 orders lower than that of 700 °C-annealed GO PD. The thermal-induced Ga/Al interdiffusion could seriously destroy the film crystallinity and result into the poor PD performance. This degraded QE performance with the increase of annealing temperature for furnace-treated GO PDs also occurs in the spectral response measurement as described in Fig. 2(c). Even though at 900 and 1000 °C, the RTA-treated GO PDs show slight decrease in QE values. The 800 °C-RTA-treated GO PD shows optimum QE performance with very small variation from 200 to 250 nm, which could benefit from both the improved crystalline quality and the suppression of diffusion by the fast thermal treatment. Note that, at very high temperature e.g., 900 and 1000 °C, even the RTA-treated GO PDs present the lower QE values. The formation of poly crystal could attribute to this phenomenon. The RTA process using 800 °C is certified as the optimum thermal treatment for the sputtered GO films on sapphire for the MSM PD application.

Various post-thermal treatments will also affect the semiconductor band structure of the sputtered GO film. Each level in the band structure can be determined and calculated from the ultraviolet photoelectron spectroscopy measurement results. Fig. 5 provides electronic structure information for β-GO films treated by furnace annealing and RTA using 800 and 1000 °C respectively. Its fermi energy level (E_F), valence band (E_V), and conduction band (E_C) show a shift tendency close to

TABLE 2
Comparison of Performance of MSM PDs Fabricated by This Work and Other Reported Gallium Oxide Films

Film	R_{max} (A/W)	I_{on} / I_{off}	T_R (s)	T_F (s)	Ref.
β-Ga_2O_3	0.553 @ 5 V	1.78×10^5	2	0.1	This work
β-Ga_2O_3	2.18 @ 50 V	4.27×10^2	0.95	1.03	[16]
β-Ga_2O_3	0.026 @ 5 V	3×10^3	1.4	0.2	[9]
β-Ga_2O_3	- @10 V	$> 10^3$	0.31	0.05	[10]
α-Ga_2O_3	0.19 @ 10 V	$> 10^4$	-	-	[17]
β-Ga_2O_3	0.004 @ 10 V	2.1×10^2	-	-	[18]
β-Ga_2O_3	0.5 @ 5 V	-	-	-	[19]
β-Ga_2O_3	1.5 @ 4 V	~1.0×10^4	3.33	0.4	[20]

the vacancy band with the increase annealing temperature from 800 to 1000 °C. Since the work function of Ti/Au is fixed, the value of SBH could be indicated by the difference of E_C and E_F. The less deviation of E_C and E_F for 1000 °C-furnace and 800 °C-RTA treated GO film proven their increased I_{dark} in Fig. 1. The RTA-treated sample shows a narrower E_F-to-F_C distance than that of the furnace-annealed one which indicates a lower SBH to overcome for photoelectron to transport from GO into Ti/Au, enhancing the PD performance. As a result, Table 2 compares the performance for the presented and other reported PDs based on sputtered GO films. Under the same bias voltage of 5 V, this work exhibits more than 21 times higher photoresponsivity than the furnace-annealed GO PD, with a nearly two orders of magnitude higher on/off current ratio [9]. Synthetically, the highest on/off current ratio, competitive photoresponsivity and fast falling time validates its applicability of RTA-treated quasi-single-crystalline GO photodetector.

4. Conclusions

The effects of various thermal treatments on sputtered GO films and their corresponding MSM PD characteristics were investigated. With the increase of treatment temperature from 700 to 1000 °C, the furnace-annealed samples processed polycrystalline structure, whereas a quasi-single-crystalline structure of the GO film can be achieved for RTA at 700 and 800 °C. The calculated bandgap of furnace-annealed samples continuously increased from 4.95 to 5.33 eV, whereas those of RTA-treated ones revealed a slight increase from 4.95 to 5.0 eV. This phenomenon could be resulted from the thermal-induced cross-diffusion of aluminum atoms tending to form $Al_xGa_{2-x}O_3$, which owned wider bandgap than the pure GO. Moreover, the furnace-annealed-GO films exhibited a degraded PD performance with the increase of annealing temperature mainly due to the thermal-induced diffusions. The RTA-treated GO films possessed better PD performance and showed optimum characteristics when annealed at 800 °C with a photo/dark current ratio of 1.78×10^5 (@ 5 V and 230 nm) and responsivity of 0.55 A/W. The highest on/off current ratio, competitive responsivity and fast falling time validates its applicability of MSM PDs from RTA-treated quasi-single-crystalline GO films. The results indicated that the sputtered GD films with proper thermal treatment have high potential for next-generation practical DUV PD applications.

References

[1] S. J. Pearton *et al.*, "A review of Ga_2O_3 materials, processing, and devices," *Appl. Phys. Rev.*, vol. 5, 2018, Art. no. 011301, doi: 10.1063/1.5006941.
[2] D. Guo *et al.*, "Zero-power-consumption solar-blind photodetector based on β-Ga_2O_3/NSTO heterojunction," *ACS Appl. Mater. Interfaces*, vol. 9, no. 2, pp. 1619–1628, 2017, doi: 10.1021/acsami.6b13771.

[3] S. Oh, J. Kim, F. Ren, S. J. Pearton, and J. Kim, "Quasi-two-dimensional β-gallium oxide solar-blind photodetectors with ultrahigh responsivity," *J. Mater. Chem. C*, vol. 4, no. 39, pp. 9245–9250, 2016, doi: 10.1039/C6TC02467J.

[4] F. Zhang, K. Saito, T. Tanaka, M. Nishio, M. Arita, and Q. Guo, "Wide bandgap engineering of $(AlGa)_2O_3$ films," *Appl. Phys. Lett.*, vol. 105, 2014, Art. no. 162107, doi: 10.1063/1.4900522.

[5] K. H. Choi and H. C. Kang, "Structural and optical evolution of Ga_2O_3/glass thin films deposited by radio frequency magnetron sputtering," *Mater. Lett.*, vol. 123, pp. 160–164, 2014, doi: 10.1016/j.matlet.2014.03.038.

[6] Y. Qin *et al.*, "High-performance metal-organic chemical vapor deposition grown ε-Ga_2O_3 solar-blind photodetector with asymmetric schottky electrodes," *IEEE Electron Device Lett.*, vol. 40, no. 9, pp. 1475–1478, Sep. 2019, doi: 10.1109/LED.2019.2932382.

[7] L. P. Dong, R. X. Jia, B. Xin, and Y. M. Zhang, "Effects of post-annealing temperature and oxygen concentration during sputtering on the structural and optical properties of β-Ga_2O_3 films," *J. Vac. Sci. Technol. A*, vol. 34. 2016, Art. no. 060602, doi: 10.1116/1.4963376.

[8] L. Huang *et al.*, "Comparison study of β-Ga_2O_3 photodetectors grown on sapphire at different oxygen pressures," *IEEE Photon. J.*, vol. 9, no. 4, pp. 1–8, Aug. 2017, Art no. 6803708, doi: 10.1109/JPHOT.2017.2731625.

[9] S. H. Yuan, C. C. Wang, S. Y. Huang, and D. S. Wuu, "Improved responsivity drop from 250 to 200 nm in sputtered gallium oxide photodetectors by incorporating trace aluminum," *IEEE Electron Device Lett.*, vol. 39, pp. 220–223, 2018, doi: 10.1109/LED.2017.2782693.

[10] J. Wang *et al.*, "High transmittance β-Ga_2O_3 thin films deposited by magnetron sputtering and post-annealing for solar-blind ultraviolet photodetector," *J. Alloy Compounds*, vol. 803, pp. 9–15, 2019, doi: 10.1016/j.jallcom.2019.06.224.

[11] L. Zhu, K. Liu, T. Z. Hu, W. Dong, Z. Chen, and Z. L. Wang, "UV-visible photocurrent enhancement using metal–semiconductor–metal with symmetric and asymmetric double Schottky barriers," *Nanoscale*, vol. 10, pp. 12848–12854, 2018, doi: 10.1039/C8NR02466A.

[12] M. Zhong, Z. Wei, X. Meng, F. Wu, and J. Li, "High-performance single crystalline UV photodetectors of β-Ga_2O_3," *J. Alloys Compounds*, vol. 619, pp. 572–575, 2015, doi: 10.1016/j.jallcom.2014.09.070.

[13] T. Huen, "Reflectance of thinly oxidized silicon at normal incidence," *Appl. Opt.*, vol. 18, no. 12, pp. 1927–1932, 1979, doi: 10.1364/AO.18.001927.

[14] Q. Hong, Y. Cao, J. Xu, H. Lu, and J. L. Sun, "Self-powered ultra-fast self-powered ultrafast broadband photodetector based on p-n heterojunctions of CuO/Si nanowire array," *ACS Appl. Mater. Interfaces*, vol. 6, pp. 20887–20894, 2014, doi: 10.1021/am5054338.

[15] L. Hu, J. Yan, M. Liao, L. Wu, and X. Fang, "Ultrahigh external quantum efficiency from thin SnO_2 nanowire ultraviolet photodetectors," *Small*, vol. 7, no. 8, pp. 1012–1017, 2011, doi: 10.1002/smll.201002379.

[16] W. Cui *et al.*, "Optimization of growth temperature of β-Ga_2O_3 thin films for solar-blind photodetectors," *J. Nanoscience Nanotechnol.*, vol. 18, no. 5, pp. 3613–3618, 2018, doi: 10.1166/jnn.2018.14692.

[17] S. J. Cui, Z. X. Mei, Y. H. Zhang, H. L. Liang, and X. L. Du, "Room temperature fabricated amorphous Ga_2O_3 high-response-speed solar-blind photodetector on rigid and flexible substrates," *Adv. Opt. Mater.*, vol. 5, 2017, Art. no. 1700454, doi: 10.1002/adom.201700454.

[18] Q. Feng *et al.*, "Comparison study of β-Ga_2O_3 photodetectors on bulk substrate and sapphire," *IEEE Trans. Electron Devices*, vol. 63, no. 9, pp. 3578–3583, Sep. 2016, doi: 10.1109/TED.2016.2592984.

[19] F.-P. Yu, S.-L. Ou, and D.-S. Wuu, "Pulsed laser deposition of gallium oxide films for high performance solar-blind photodetectors," *Opt. Mater. Exp.*, vol. 5, no. 5, pp. 1240–1249, 2015, doi:10.1364/OME.5.001240.

[20] A. Singh Pratiyush *et al.*, "High responsivity in molecular beam epitaxy grown β-Ga_2O_3 metal semiconductor metal solar blind deep-UV photodetector," *Appl. Phys. Lett.*, vol. 110, 2017, Art. no. 221107, doi: 10.1063/1.4984904.